SANDIA REPORT

SAND2013-10574
Unlimited Release
October, 2013

Non-Abelian Fractional Quantum Hall Effect for Fault-Resistant Topological Quantum Computation

W. Pan, M. Thalakulam, X. Shi, M. Crawford, E. Nielsen, and J.G. Cederberg

Prepared by
Sandia National Laboratories
Albuquerque, New Mexico 87185 and Livermore, California 94550

Sandia National Laboratories is a multi-program laboratory managed and operated by Sandia Corporation, a wholly owned subsidiary of Lockheed Martin Corporation, for the U.S. Department of Energy's National Nuclear Security Administration under contract DE-AC04-94AL85000.

Issued by Sandia National Laboratories, operated for the United States Department of Energy by Sandia Corporation.

Available to DOE and DOE contractors from
U.S. Department of Energy
Office of Scientific and Technical Information
P.O. Box 62
Oak Ridge, TN 37831

Telephone: (865) 576-8401
Facsimile: (865) 576-5728
E-Mail: reports@adonis.osti.gov
Online ordering: http://www.osti.gov/bridge

Available to the public from
U.S. Department of Commerce
National Technical Information Service
5285 Port Royal Rd.
Springfield, VA 22161

Telephone: (800) 553-6847
Facsimile: (703) 605-6900
E-Mail: orders@ntis.fedworld.gov
Online order: http://www.ntis.gov/help/ordermethods.asp?loc=7-4-0#online

SAND2013-10574
Unlimited Release
October, 2013

Non-Abelian Fractional Quantum Hall Effect for Fault-Resistant Topological Quantum Computation

Wei Pan, Madhu Thalakulam, Xiaoyan Shi, Matthew Crawford, Erik Nielsen
Quantum Phenomena Department

Jeff G. Cederberg
Advanced Materials Sciences Department

Sandia National Laboratories
P.O. Box 5800
Albuquerque, New Mexico 87185-MS1086

Abstract

Topological quantum computation (TQC) has emerged as one of the most promising approaches to quantum computation. Under this approach, the topological properties of a non-Abelian quantum system, which are insensitive to local perturbations, are utilized to process and transport quantum information. The encoded information can be protected and rendered immune from nearly all environmental decoherence processes without additional error-correction. It is believed that the low energy excitations of the so-called $\nu=5/2$ fractional quantum Hall (FQH) state may obey non-Abelian statistics. Our goal is to explore this novel FQH state and to understand and create a scientific foundation of this quantum matter state for the emerging TQC technology.

We present in this report the results from a coherent study that focused on obtaining a knowledge base of the physics that underpins TQC. We first present the results of bulk transport properties, including the nature of disorder on the 5/2 state and spin transitions in the second Landau level. We then describe the development and application of edge tunneling techniques to quantify and understand the quasiparticle physics of the 5/2 state.

.

ACKNOWLEDGMENTS

CONTENTS

FIGURES

1. INTRODUCTION

The most secure modern encryption method is based on the assumption that it is impossible to prime-factorize a large digit number within a reasonable time frame. Indeed, it is estimated that factorizing a 200-digit number would require 170 CPU years using an Intel computer. This estimate, however, is drastically changed with the use of a quantum computer. In a paper published in 1994 by Peter Shor, he showed that a quantum computer (QC) could readily factorize a 300-digit number. This began a world-wide interest in QC research. Yet, after 15 years of research, many fundamental issues remain unresolved. For example, the strong coupling between electrons and their *local* environments greatly reduces electron coherence time and requires complex error-correction schemes to manipulate quantum information before it is lost. As such, there is a pressing need to identify new paradigms which can potentially enable revolutionary advances in the field of quantum computation.

Topological quantum computation (TQC) has emerged as one of the most promising approaches. Under this approach, the *topological* properties of a non-Abelian quantum system, which are insensitive to local perturbations, are utilized to process and transport quantum information. The encoded information can be protected and rendered immune from nearly all environmental decoherence processes without additional error-correction. It is now generally believed that the low energy excitations of the so-called $\nu=5/2$ fractional quantum Hall (FQH) state may obey non-Abelian statistics. Our goal is to explore this novel FQH state and to understand and create a scientific foundation for exploiting this quantum matter state in order to build a knowledge base for the emerging TQC technology.

In this LDRD research, we propose to carry out a coherent study to obtain a scientific foundation of TQC. Success of this project is expected to have a great impact on the feasibility of eventually building a topological computer.

Our proposed work is based on our world-leading research in the fractional quantum Hall (FQH) physics. We will study the physics of the 5/2 ground state; the elementary excitations of the 5/2 state and their transport properties; and the quantum interference of these elementary excitations that might be relevant to constructing a quantum bit (or, in short, qubit).

2. NATURE OF DISORDER MATTERS IN THE 5/2 FRACTIONAL QUANTUM HALL EFFECT

Among all observed fractional quantum Hall effect (FQHE) [1,2] states, the $\nu=5/2$ FQHE state [3,4] in the second Landau level remains the most exotic one. This state has been at the center of current quantum Hall research due to the possibility of it being non-Abelian [5,6] and, thus, having potential applications in fault-tolerant topological quantum computation [7].Therefore, there is an urgent need to understand the impact of disorder on this FQHE state, since a larger energy gap at $\nu=5/2$ would exponentially reduce error rates [7] and make the envisioned quantum computation more robust.

Today, our knowledge of the impact of various kinds of disorder on the 5/2 FQHE, or any other of the FQHE states, remains limited. Indeed, it has long been observed [8,9] that in the lowest Landau level, even after taking into account the finite thickness correction of 2DES and Landau level mixing effect, there is still a discrepancy of ~ 2-3K between the experimentally measured energy gaps of the odd-denominator FQHE states and theoretically calculated ones. This value of discrepancy has also been observed for the 5/2 state and the odd-denominator FQHE stats in the second Landau level [4]. In order to reconcile the discrepancy, often, a very vague quantity termed "disorder broadening" is employed [4], which does not seem to correlate with the 2DES mobility. Moreover, little is known about the nature of disorder, e.g., the different influence of long range Coulombic and short range neutral disorders, on the energy gap.

On the other hand, understanding the impact of disorder is essential for understanding the nature of a quantum system. As shown in a series of papers [10], the long standing controversies on the universality of quantum Hall plateau transition is directly linked to the nature of disorder in the 2D channel. In 2DES samples with strong disorder from a short-range neutral alloy potential a perfect power law scaling behavior of quantum Hall plateau-to-plateau transition was observed over more than two decades of temperatures, from 1.2K down to 10 mK. In contrast, in samples with weak disorder from a long-range Coulombic potential a crossover behavior was observed from a non-universal scaling region at high temperatures to a universal scaling region at low temperatures.

In this section, we present our results on how the nature of disorder affects the 5/2 energy gap and, thus, the stability of this state. We compare the activation energy gap data obtained in two types of samples: symmetrically doped modulation quantum well samples and undoped heterojunction insulate-gated field-effect transistors (HIGFETs). In modulation doped quantum well samples, where long-range Coulombic disorder dominates, the energy gap drops quickly with decreasing mobility (or increasing disorder). On the other hand, in HIGFET samples, where the short-range neutral disorder dominates, the 5/2 energy gap shows only a weak mobility dependence. Our results clearly demonstrate that the two types of disorder play very different roles in affecting the stability of the 5/2 state. Possible physical mechanisms are discussed.

For this study we used two HIGFET (heterojunction insulate-gated field-effect transistor) [11] devices, called A and B. Results from these two samples are consistent with each other. Figure 1 shows the mobility (μ) versus electron density (n) obtained in HIGFET A. The mobility first increases with increasing n, reaches a peak of $\mu \sim 14 \times 10^6$ cm^2/Vs around n ~ 1.8×10^{11} cm^{-2}, and then decreases with increasing n. The decrease of mobility with increasing density beyond n ~ 1.8×10^{11} cm^{-2} is due to surface roughness scattering [12], which is of short-range. The weak kink at n ~ 3.5×10^{11} cm^{-2} is probably due to the onset of occupation of the second electrical subband.

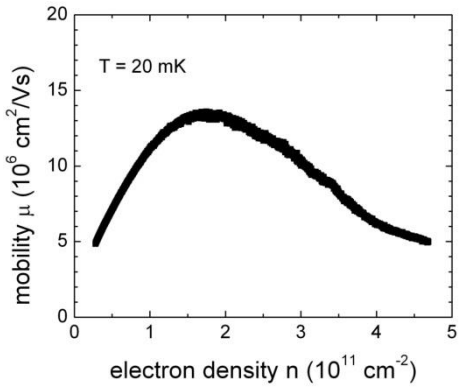

Figure 1: Electron mobility versus density in HIGFET A.

We studied the ν=5/2 state at various densities. In Figure 2a, we show the data obtained in HIGFET B, taken at the high B/T facilities of National High Magnetic Field Laboratory at the University of Florida. Different from the conventional magneto-transport measurement, where the 2D electron density is fixed and the magnetic field is swept, here, the magnetic field is fixed and the gate voltage and hence the carrier densities is swept. This process minimizes heating from eddy currents. As shown in Figure 2a, a well-developed 5/2 state is observed and its diagonal resistance (R_{xx}) minimum reaches a very low value of ~ 10 ohms at a density of n=2.85×10^{11} cm^{-2}. With decreasing electron density, R_{xx} at ν=5/2 increases, but the minimum remains visible down to n ~ 0.55×10^{11} cm^{-2}.

The density dependence of the 7/3 state is similar to that of the 5/2 state. However, the 8/3 state shows a slightly different density dependence. Its strength first decreases with decreasing density and then seems to saturate at lower densities.

Figure 2b shows the R_{xx} traces at a few selected temperatures taken at a magnetic field B = 4.68T. Clearly, the R_{xx} minimum shows an activated behavior, i.e., R_{xx} increases with increasing temperature. This is different from our previous study [13] and thus allows us to obtain an activation energy value for the 5/2 state, as shown in Fig.2c.

In Fig. 2d, we show the density dependence of the 5/2 energy gap in HIGFET A, in the density range where surface roughness dominates. In this density range, the 5/2 energy gap increases with increasing 2D electron densities. Two important features are apparent: 1) the increase of the 5/2 energy gap is not caused by an increase in electron mobility.

The energy gap at ν=5/2 increases by a factor of more than 3 from ~0.07 K at n ~1.8×10^{11} cm^{-2} to 0.24 K at ~4×10^{11} cm^{-2}, while over the same density range the mobility actually decreases by a factor of 2. 2) the dependence of the energy gap on density is smooth and no sharp features are apparent.

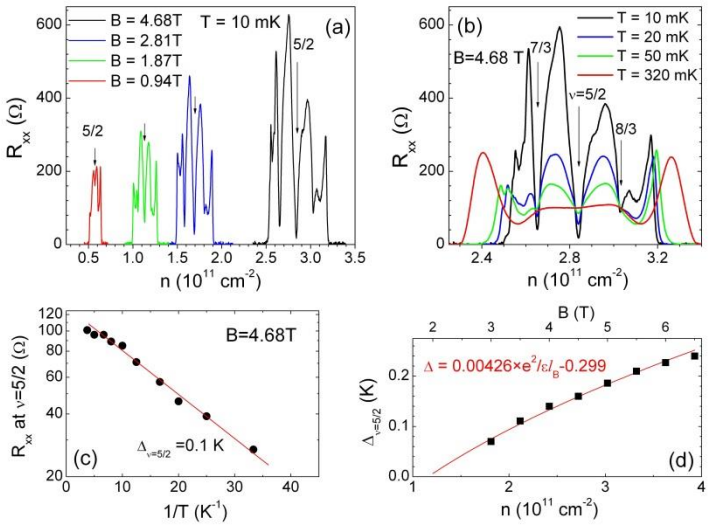

Figure 2: FQHE states in diagonal magneto-resistance around ν=5/2 in HIGFET B. (a) R_{xx} versus n at various magnetic fields. (b) Temperature dependence at B = 4.68T. (c) Arrhenius plot for the R_{xx} minimum at ν=5/2 at B = 4.68T. The line is a linear fit to the data. An energy gap of ~ 0.1K is obtained from the slope of this linear fitting. (d) Density dependence of the 5/2 energy gap in HIGFET A. The bottom x-axis is electron density, the top magnetic field. The red line is a fit according to a spin polarized model.

To better appreciate the impact of disorder on the 5/2 state, we plot in Figure 3a the normalized 5/2 energy gap versus electron mobility (measured at zero magnetic field) for HIGFET A. The normalized energy gap, defined by $\Delta_{\nu=5/2}/e^2/\varepsilon l_B$, is used to eliminate the density dependence of the energy gap in different samples. For comparison, we include in Fig.3a our 5/2 energy gap data from high quality, symmetrical modulation-doped 30nm quantum wells reported in Ref. [14]. Due to the wide well width, the disorder in such quantum wells is expected to be dominantly by distant ionized impurities and hence long-ranged. We further include the results by other groups [15-20], again in modulation doped quantum wells with the same or even larger well width in which the disorder is expected to be also long-ranged. Only the high density data points in Ref. [19] are used. In Fig. 3b, the data of Fig. 2 are plotted as a function of 1/μ, which is a rough measure of sample disorder. It is clear that the two types of samples, HIGFETs and quantum-wells, show very different mobility dependences. For the modulation doped samples, where sample disorder is of long range, the normalized energy gap decreases sharply with decreasing mobility or increasing disorder. An apparent mobility threshold for a non-zero 5/2 energy gap of ~10×10^6 cm^2/Vs, is obtained from the extrapolation of a linear fit. On the other hand, in the HIGFET where the disorder is dominantly caused by charge-neutral

surface roughness scattering, which is of short-range, a weak mobility dependence is seen. In fact, the normalized energy gap increases slightly with decreasing mobility or increasing disorder. This contrasting behavior suggests that the long-ranged Coulombic and short-ranged charge-neutral disorders play very different roles in affecting the 5/2 energy gap.

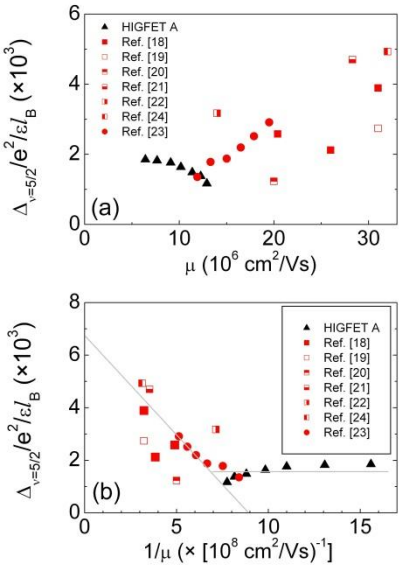

Figure 3: (a) normalized 5/2 energy gap, $\Delta_{\nu=5/2}/e^2/\varepsilon l_B$, as a function of μ; and (b) as a function of 1/ μ for HIGFET A and modulation doped quantum well samples. The two lines in (b) are guides to the eye.

Before we discuss possible mechanisms that may be responsible for the observed difference, let us first look at the finite thickness effect of 2DES. We calculated the thickness of the 2DES using the self-consistent method for the symmetric quantum wells and the Fang-Howard wavefunction for the HIGFETs. For the majority of the QWs quoted in our paper, the effective thickness, define by w/l_B, is roughly the same, $w/l_B \sim 2$. Here w is the finite thickness of the 2DES in the growth direction and l_B the magnetic length at ν=5/2. For the HIGFETs, due to the fact that w scales as $n^{-1/3}$ and $l_B \propto n^{-1/2}$, $w/l_B \propto n^{-1/6}$ shows a much weaker density dependence. In our studied density range, it varies between 0.9 and 1.1. We notice that in a recent paper [21] the change in the overlap between the exact wavefaction and the Pfaffian model wavefunction is smooth and the difference is small as w/l_B varies from 1 to 2. Thus, it is hard to imagine that this factor of 2 difference in our samples can present such a striking difference in the disorder dependence observed in our experiment.

In the following, we discuss several possibilities that may shed some light on our understanding of the origin of the observed difference in the mobility dependence. One possibility is that the attractive Coulombic interaction between ionized donors in the doping layer and 2D electrons may affect the pairing of composite fermions [22,23] at ν

=5/2. Indeed, it is known that Coulomb interaction can cause fluctuations of the phase of the superconducting order parameter and, therefore, destroy superconductivity [24]. Recent studies by Umansky et al [25] and Gamez et al [26] also showed the importance of ionized dopants in suppressing the development of the 5/2 state as well as other quantum Hall states in the second and higher Landau levels.

A second possibility might be related to the size of the quasi-particles at ν =5/2. In a recent study by Nübler et al [19], it was shown that the size of 5/2 quasiparticles is fairly large, ~ 10 magnetic length, or ~ 0.1 μm or larger in our density range. Such large size quasiparticles may not be affected at all by the nanometer or sub-nano meter size fluctuations from surface roughness, whereas the long-range fluctuations from remote impurities might assembles the quasi particles into poorly connected puddles of micron size, which affect macroscopic transport and hence the energy gap data.

We also want to address an earlier discussion [27] on long-range and short-range disorder potentials in affecting the bounded magneto-rotons [28,29] and the current carrying quasiparticles near impurities. It was argued [27] that around impurities the ground state was slightly deformed. Such a deformation is energetically less costly if rotons are being excited, which in turn affect the energy gap of a FQHE state. It is possible that in the presence of long range disorder, such deformations in the 5/2 ground state occurs around the perimeter of electron puddles. As a result, its energy gap is expected to depend on the puddle size, which, in long-range potentials such as the one created by remote impurities of quantum-well samples, is related to electron mobility. In HIGFET samples, on the other hand, the mobility is dominated by short range potential fluctuations from surface roughness and this disorder configuration is largely fixed after sample growth. Therefore, in this case, a weak mobility dependence on the 5/2 energy gap as the 2DES density is varied, is not unexpected.

Finally, our data also can shed some light on the controversy between the 5/2 state being spin polarized or spin-unpolarized. The red line in Fig.2d shows our best fit assuming a fully polarized ground state at ν=5/2, with Δ given by $\Delta = \alpha e^2/\varepsilon l_B - \Gamma$. Here, e is the electron charge, l_B is the magnetic length, ε is the dielectric constant of GaAs, Γ is the disorder broadening, and α is a variable. The finite layer-thickness [21,30] and Landau level mixing effects [19,31,32] were not taken into account. The optimum parameters turn out to be α=0.00426 and Γ = 0.23, with α being quite similar to the one we obtained previously [16]. Fitting according to a spin-unpolarized ground state model (i.e., $\Delta = \alpha e^2/\varepsilon l_B - g^*\mu_B B - \Gamma$, where the effective g-factor for GaAs g* = 0.44 and μ_B is the Bohr magneton) yields a much worse result. Indeed, the reduced χ^2 obtained from the two fittings differs by almost a factor of 10 -- 0.00004 in spin-polarized fitting versus 0.0003 in spin-unpolarized fitting. This then suggests that our density dependent result of the 5/2 energy gap support a spin polarized 5/2 state.

In summary, we have examined the impact of different kind of disorders on the experimental 5/2 energy gap. We observe that in modulation doped quantum well samples where disorder is dominated by the long-range Coulombic fluctuations the 5/2 energy gap decreases quickly with increasing 1/μ or disorder. On the other hand, in

HIGFETs, where the disorder is dominantly due to short-range surface roughness fluctuations, the 5/2 energy gap shows a weak mobility dependence. Moreover, our density dependent result of the 5/2 energy gap is consistent with a spin polarized 5/2 state and deviates considerably from a description in terms of a spin-unpolarized state.

3. SPIN POLARIZATION OF THE 12/5 FRACTIONAL QUANTUM HALL EFFECT

In recent years, the 12/5 state has attracted growing interest [33-43] due to its superior potential in performing universal topological quantum computation than the 5/2 state [44,45]. On the other hand, in contrast to the well-documented 5/2 state, much less experimental work has been carried out on this state, partially due to its very fragile nature and an extremely small energy gap. Up to date, except for the observation of a well-developed quantum Hall plateau at this filling [46,20] there is no direct experimental evidence to support this state being a parafermionic or non-Abelian state.

In this section, we present our tilt magnetic field dependence results in examining the spin-polarization of the 12/5 state. It was observed that the diagonal magneto-resistance R_{xx} at ν=12/5 shows a non-monotonic dependence on tilt angle θ. It first increases sharply with increasing θ, reaching a maximal value of ~ 70 Ω around $\theta \sim 14^o$ (at which the total B field $B_{total} = B_{perp}/\cos(\theta) = 4.8$T.). R_{xx} then decreases with further increase of θ. Correlated with this dependence of R_{xx} on θ at ν=12/5, the 12/5 activation energy ($\Delta_{12/5}$) also shows a non-monotonic dependence. $\Delta_{12/5}$ first decreases with increasing θ and vanishes around $\theta = 14^o$, when R_{xx} becomes non-activated. With further increasing tilt angles, R_{xx} becomes activated again and $\Delta_{12/5}$ increases with θ. This tilt B dependence of R_{xx} at ν=12/5 and of $\Delta_{12/5}$ are similar to the composite fermion FQHE states at ν = 2/5 and 8/5 in the lowest Landau level, which now is generally believed to be due to a spin transition. Our results thus call for more investigations on the nature of the 12/5 ground state.

The ultra-high quality 2DES specimen we used in this experiment is a symmetrically doped $Al_{0.24}Ga_{0.76}As/GaAs/Al_{0.24}Ga_{0.76}As$ quantum well (QW). The well width is 30 nm and the set-back distance is 80 nm on both sides of QW. The low temperature 2DES density $n = 2.7\times10^{11}$ cm^{-2} and mobility $\mu = 31\times10^6$ cm^2/Vs were established after a red light-emitting-diode illumination for several hours at T ~ 4.2K. The size of the sample is about 4 mm × 4 mm with eight indium contacts placed symmetrically around the edges, four at the sample corners and four in the center of the four edges. Our ultralow temperature measurements were conducted in the same setup as in Ref. [47], where the sample can be tilted in-situ by a hydraulic ^{3}He rotator. During the tilting process, the perpendicular B field (B_{perp}) is fixed for each Landau level filling, while the total B field increases with increasing tilt angle according to $B_{total} = B_{perp}/\cos(\theta)$. The in-plane B field is aligned with [110] crystal direction. Standard low-frequency lock-in technique is utilized to measure the diagonal resistance R_{xx} (the excitation current perpendicular to the in-plane B field when under tilt), R_{yy} (current parallel to in-plane B field) and Hall resistance R_{xy}. The measurement frequency is ~ 8 Hz and the excitation current is 2-5 nA. During the course of this experiment, the same specimen was thermally recycled from room temperature to the fridge base temperature four times. Data from each cool-down are consistent with each other.

Figure 4 shows the R_{xx} trace taken at the first cool-down at a fridge temperature of ~ 20 mK. In this high quality specimen, well developed FQHE states are observed at ν=14/5(2+4/5), 8/3(2+2/3), 5/2, 7/3(2+1/3), 16/7(2+2/7), and 11/5(2+1/5), evidenced by strong R_{xx} minima and quantized Hall plateaus (as shown in the R_{xy} trace at $\theta = 0°$ in Fig.5). Developing FQHE states are also observed at ν=19/7(2+5/7), 12/5(2+2/5), 19/8(2+3/8). The observation of these states is consistent with previous work. Besides the above now-generally accepted FQHE states, R_{xx} minima are also observed on both sides of the 5/2 state at B ≈ 4.41T and 4.53T. The one at B ≈ 4.53T can be assigned to the Landau level filling of ν=2+6/13, consistent with a previous study [20]. Surprisingly, in this sample, a quite strong R_{xx} minimum is also observed at ν=21/8(2+5/8), the particle-hole conjugate state of the ν=19/8(2+3/8) state. However, this minimum disappears in the R_{yy} trace. It is not clear at the present time whether this disappearance of R_{yy} is extrinsic (such as due to non-perfect ohmic contacts) or intrinsic (such as due to the formation of an anisotropic phase [48] at this filling). Furthermore, between B = 4.9 and 5.0T, there are three R_{xx} local minima. The two at B = 4.92 and 5.00T correspond to the Landau level fillings ν= 25/11(2+3/11) and 29/13 (2+3/13), respectively. The third minimum at 4.95T, however, is not at any apparent rational filling factor even through it is close to 9/4 (2+1/4). All these three minima disappear in the R_{yy} trace. Further studies are needed to clarify the origins of these new minima.

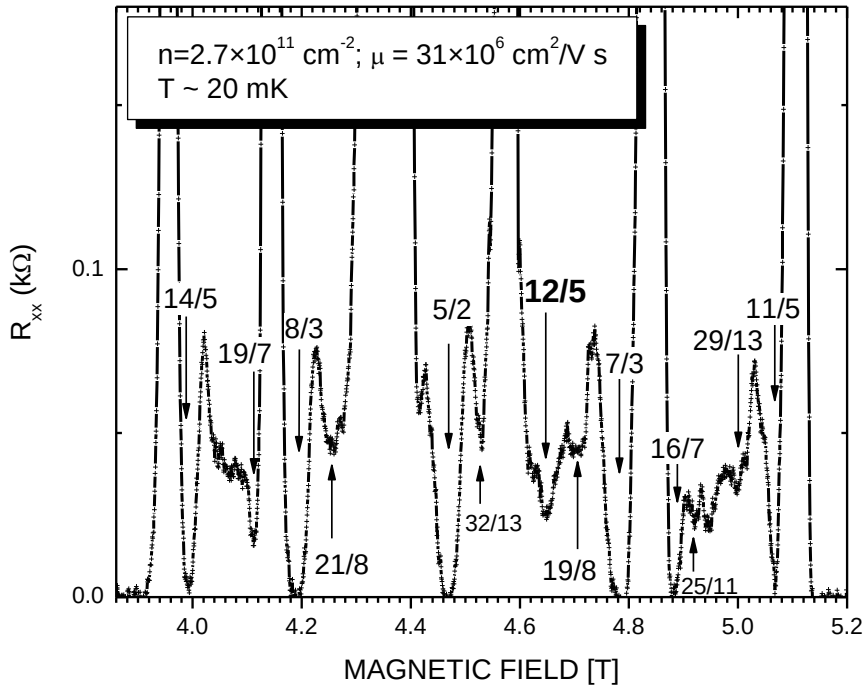

Figure 4 R_{xx} trace taken at $\theta = 0°$ under perpendicular magnetic fields. The arrows mark the fractional quantum Hall states at ν = 14/5, 19/7, 8/3, 5/2, 32/13, 12/5, 19/8, 7/3, 16/7, and 11/5. Local minima are also observed at ν=21/8, 25/11, and 29/13. The minimum at B = 4.95T is close to ν=9/4. These four minima disappear in the R_{yy} trace.

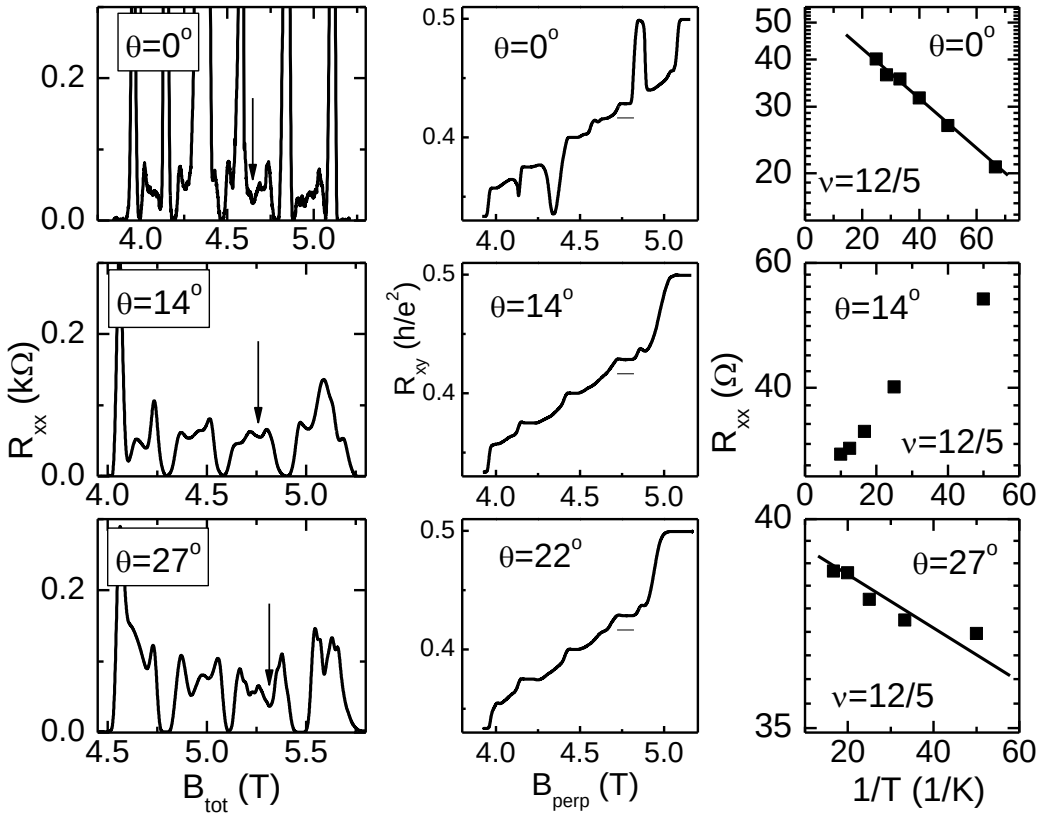

Figure 5 The left column shows the R_{xx} traces at three selected tilt angles, $\theta = 0^o$, 14^o, 27^o. The arrows mark the positions of the 12/5 state. The middle column shows the corresponding R_{xy} traces at $\theta = 0^o$, 14^o, and 22^o, respectively. The horizontal lines show the expected Hall value of the 12/5 state. The right column shows in semi-log plot the R_{xx} versus $1/T$ at ν=12/5 at $\theta = 0^o$, 14^o, and 27^o. Lines are linear fit.

In the left column of Figure 5, R_{xx} traces are displayed at three selected angles, $\theta = 0°$, 14°, and 27°. The 12/5 state first becomes weaker with increasing tilt angle (shown for θ = 14°), but it becomes a little bit stronger as the tilt angle is further increased (θ = 27°). This trend is corroborated in the R_{xy} plot and the temperature dependence of R_{xx}. Shown in the middle column, at $\theta = 0°$, a Hall plateau is clearly visible at ν=12/5. At θ = 14°, the plateau disappears and R_{xy} displays roughly linear B dependence. As the tilt angle is further increased to θ = 22°, a kink starts to develop at ν=12/5. The temperature dependence data is shown in the right column. At $\theta = 0°$, R_{xx} is activated. Though the change of R_{xx} is small over the temperature range, nevertheless, an activation energy $\Delta_{12/5}$ can be obtained from fitting the data according to $R_{xx} \propto \exp(-\Delta_{12/5}/2k_BT)$, and $\Delta_{12/5} \sim 30$ mK. At θ = 14° degrees, the R_{xx} does not show an activated behavior. Instead, R_{xx}

decreases with increasing temperature. As θ continues to increase to θ = 27°, R_{xx} becomes activated again, albeit the activation energy at this tilt angle is much smaller, ~ 3mK. Before we discuss Fig. 6, we want to point out that the four huge magnetoresistance peaks associated with the re-entrant integer quantum Hall effect [15] disappear quickly as the specimen is tilted away from the sample normal, a phenomenon first reported in Ref. [47].

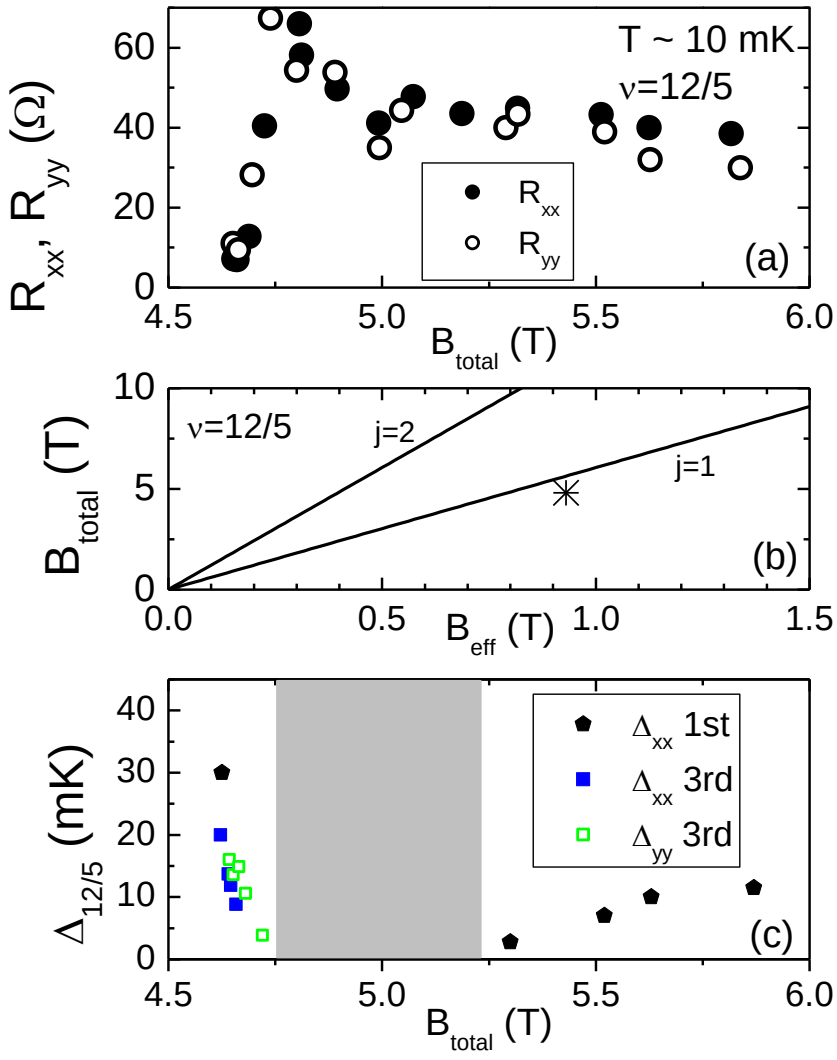

Figure 6 (a) R_{xx} and R_{yy} at ν=12/5 versus B_{total}, measured at T ~ 10 mK in the second cool-down. (b) B_{total} versus B_{eff} plot for the maximum at B_{total} = 4.8T in (a). The star is the experimental data point. The lines are for $B_{total}/B_{eff} = j \times 2m_e/(g^*m^*)$ with j=1 and 2, respectively. (c) $\Delta_{12/5}$ as a function of B_{total} from two cool-downs. For the third cool-down, $\Delta_{12/5}$ from the temperature dependence of both R_{xx} and R_{yy} is shown. In the gray region, magneto-resistance is not activated and $\Delta_{12/5}$ is not obtainable.

In Figure 6a, the R_{xx} and R_{yy} values at $\nu=12/5$ are plotted as a function of B_{total}. The data were taken at the base temperature of ~ 10 mK in the second cool-down. Two features need to be emphasized. First, in the studied tilt angle range, the values of R_{xx} and R_{yy} are roughly the same. The tilt induced anisotropic electron transport is not observed. Second, the diagonal magneto-resistance shows non-monotonic tilt B field dependence. It first increases sharply from a value of ~ 7 Ω at $\theta = 0°$ to a maximum of ~ 70 Ω at $\theta \sim 14°$. With further increasing θ, R_{xx} and R_{yy} decrease gradually to ~ 35 Ω at $\theta \sim 40°$.

In Figure 6c, the 12/5 activation energy data from two cool-downs are displayed. It also shows a non-monotonic B_{total} dependence. $\Delta_{12/5}$ decreases quickly from ~ 30 mK at $\theta = 0°$ to ~ 5 mK at $\theta = 10°$. Between $\theta \sim 10°$ and 25° (the gray region), where the curve of R_{xx} (R_{yy}) *vs.* B_{total} displays a broad peak, the magneto-resistance is non-activated. As a result, $\Delta_{12/5}$ can not be deduced. Beyond $\theta = 27°$, $\Delta_{12/5}$ re-emerges and increases with increasing tilt angles.

The tilt angle dependence of the R_{xx} (R_{yy}) at $\nu=12/5$ and $\Delta_{12/5}$ is reminiscent of a spin unpolarized ground state under tilt. Indeed, the B_{total} dependence of R_{xx} is very much like that at $\nu=8/5$ [49] and the trace of $\Delta_{12/5}$ versus B_{total} is similar to those of the 8/5 and 2/5 states in the lowest Landau level [50,51]. For both the 2/5 and 8/5 states, the non-monotonic tilt dependence is now generally accepted to be due to a spin transition from a spin unpolarized state to a spin polarized state. In this regard, our tilt magnetic field dependent results indicate a similar spin transition in the 12/5 state.

If this is the case, then, our results apparently are inconsistent with the theoretical models proposed for the 12/5 state being a spin-polarized FQHE state. Rather, they call for the 12/5 state be described as an integer quantum Hall state of non (or weakly) interacting CFs in the second Landau level where it is mapped onto the $\nu^*=2$ state. We show in Fig.3b our fitting according to the model of CFs with a spin. Following the procedure used in Ref. [49], we construct the plot of B_{total} versus B_{eff}, where B_{eff} is the effective magnetic field in the second Landau level. For the 12/5 state, $B_{eff} = 5\times(B_{12/5}-B_{5/2}) = 0.93$T. Here, $B_{12/5}$ and $B_{5/2}$ are the perpendicular B field at $\nu=12/5$ and 5/2, respectively. The lines are for $B_{total}/B_{eff} = j\times 2m_e/(g^*m^*)$, where the crossing of CF Landau levels of different spins occurs. $j=1,2,\ldots$ is an integer number. g^* and m^* are the effective g-factor and mass of the CFs in the second Landau level. To our knowledge, neither experimental measurements nor theoretical calculations have been reported on these two parameters. On the other hand, since the effective mass follows an empirical relationship of $m^*/m_e \approx 0.26\times B_\nu^{1/2}$ for the CFs in the lowest Landau level [52], we assume that this relationship also holds for the CFs in the second Landau level. Consequently, $m^* = 0.55m_e$ is obtained. For g^*, we use the value of 0.6, which has been measured at various even-denominator fillings in the lowest Landau level [53]. With these two values, the lines for $j=1$ and 2 are drawn in Fig. 6b. It is clearly seen that the peak position in the plot of R_{xx} (R_{yy}) versus B_{total} (Fig. 6a) corresponds to the CF Landau level crossing with $j=1$, just like the 8/5 state in the lowest Landau level [49] and, therefore, strongly supporting the 12/5 state being an IQHE state of CFs.

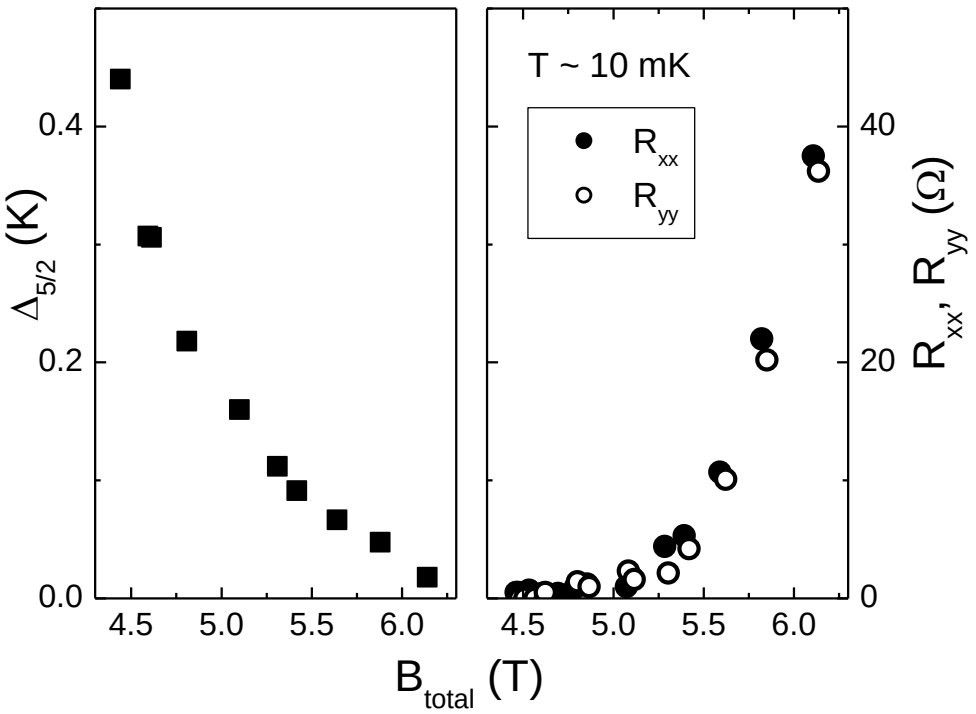

Figure 7 (a) The energy gap of the 5/2 state as a function of B_{total}. (b) R_{xx} and R_{yy} at ν=5/2 versus B_{total}, measured at T ~ 10 mK.

It is interesting that the non-interacting CF model provides a highly plausible explanation to the tilt B field dependent data in Fig. 5a. On the other hand, the apparent agreement may also signal a new exotic correlated state of composite fermions with spin in the 12/5 FQHE, which allows Zeeman engineering between an unpolarized state (its origin unknown but could be a spin singlet non-Abelian state [34]) and a polarized state (possibly a parafermionic state). In this regard, we do notice that there are a couple of experimental observations that are inconsistent with the CF model. In general, one expects to see a gap opening right after the LL crossing. This is not observed in Fig. 6c, where there exists a fairly large region where R_{xx} remains non-activated and a true activation gap is not obtainable. Second, the increase of $\Delta_{12/5}$ as a function B_{total} is much weaker after $\Delta_{12/5}$ reappears, when compared to the decreasing rate in the small tilt angle regime. This is different from the 8/5 and 2/5 states, where a similar magnitude was observed before and after the collapse of energy gap [50,51]. At the present time, there is no concrete explanation for this discrepancy. One possibility is that there is no spin transition in the 12/5 FQHE. Instead, the non-monotonic angular dependence could be due to a more complicated mechanism, such as a quantum phase transition from a non-Abelian parafemionic state at zero tilt to an exotic quantum state at high tilt angles. In fact, our very preliminary results show that in the high tilt regime the $\Delta_{12/5}$ value from the temperature dependence of R_{yy} is different from that of R_{xx}, suggesting possibly a co-

existence phase of the FQHE liquid state with an anisotropic state [54]. Another possibility is that the small slope in the high tilt angle regime is due to that the 12/5 state being in the different electrical subband. In this regard, we have carried out a self-consistent calculation for our sample. It is observed in our tilt range in Fig.6 the 12/5 state (as well as the 5/2 state) remains in the second Landau level of the lowest electrical subband and energetically is far away from the low Landau level of the second electrical subband (however, we note here that the coupling between the electrical bands and magnetic Landau levels under tilt was not considered in the self-consistent calculations.). Moreover, it is clear that in Fig. 7a $\Delta_{5/2}$ decreases continuously with increasing tilt angles and there is no large change in the 5/2 energy gap, as observed by Liu *et al* [55] when the two electrical subbands cross each other.

Finally, it is interesting to observe that the tilt magnetic field induced anisotropic phase was not observed at $\nu=5/2$ in this sample, and R_{xx} and R_{yy} are more or less the same even when the 5/2 FQHE state is destroyed at $\theta \sim 40°$, as shown in Figure 7b. This isotropic tilt B field dependent behavior at $\nu=5/2$ has also been observed in previous work [56]. The exact origin remains unknown at the present time.

To summarize, we have carried out tilt magnetic field dependent studies of the 12/5 fractional quantum Hall effect state. Its diagonal magneto-resistance R_{xx} shows a non-monotonic dependence on tilt angle, and displays a maximum at $\theta \sim 14°$. We show that this tilt dependence can be understood within the model of CFs with a spin, with appropriate m* and g* values assumed. Furthermore, correlated with the tilt dependence of R_{xx} and R_{yy}, the 12/5 activation energy $\Delta_{12/5}$ also shows a non-monotonic B dependence. This tilt B dependence of R_{xx} and $\Delta_{12/5}$ is in striking difference from that of the well-documented 5/2 state and, thus, calls for more investigations of the nature of the 12/5 FQHE.

4. SPIN TRANSITION IN THE ν=8/3 FRACTIONAL QUANTUM HALL EFFECT

The fractional quantum Hall effect (FQHE) [1,2] in the second Landau level has attracted a great deal of interests in recent years due to its possible applications in fault-resistant topological quantum computation [7]. Tremendous advance has been achieved in understanding the most celebrated 5/2 FQHE state, believed to be due to paring [5] of composite fermions (CF) [57-59] and that its elementary excitations obey non-Abelian statistics.

In addition to the 5/2 state, many odd-denominator FQHE states have also been observed, for example at Landau level fillings ν=7/3 and 8/3[3,4,14-20,46,55,60,61]. In contrast to the 5/2 state, much less work has been carried out for these states. On the other hand, unlike the odd-denominator FQHE state in the first Landau level, where most of them are well understood within the picture of either the hierarchical model [62,63] or CF model [57-59], the nature of the odd-denominator FQHE states in the second Landau level remains largely unsettled [64]. This is even true for the most prominent ones at the simplest odd-denominator Landau level fillings ν=7/3 and 8/3. Indeed, a Laughlin type FQHE state was originally ruled out for these two states based on finite size, few particles calculations [65,66]. More recent detailed calculations have also shown that the model of weakly interacting composite fermions is not adequate for these second Landau level fractions [64]. Over the years, proposals of novel ground states [27-37] have been put forward. It is expected that a deep understanding of the FQHE in the second Landau level will lead to much exciting many-body physics [64].

Experimentally, currently available transport results appear more complex than expected from a simple analogy of their counterparts (the ν=1/3 and 2/3 FQHE states) in the first Landau level. For example, it has been observed by many groups that the energy gap of the 7/3 state is roughly two times that of the 8/3 state. This difference cannot be explained by assuming these two states are particle-hole conjugate states and, thus, by the slight difference in *B*-field at ν=7/3 and ν=8/3. As a result, an explanation related to spin polarization was proposed [14]. Naively, extrapolating from the lowest Landau level, one might expect that the 7/3 state is spin polarized, whereas the 8/3 state is unpolarized. However, one earlier theoretical paper [71] predicts that the ν=8/3 state is also spin-polarized even at vanishingly small Zeeman energies.

To study the spin-polarization of a FQHE state, the commonly used experimental technique is to tilt sample in-situ in magnetic fields at very low temperatures [72-74]. By so doing, one varies the relative strength of the Zeeman energy (E_z) and the Coulomb energy (E_c), where $E_z = g^*\mu_B B_{total}$ and $E_c = e^2/\varepsilon l_B$. g*=0.44 is the effective g-factor, μ_B the Bohr magneton. $B_{total} = B_{perp}/\cos(\theta)$ is the total magnetic field under tilt, B_{perp} the perpendicular magnetic field to the sample normal and θ the tilt angle. $l_B = (\hbar/eB_{perp})^{1/2}$ is the magnetic length, ħ the Planck constant, e the electron charge. ε is the dielectric constant of GaAs. However, this technique appears to be complicated to tackle the spin polarization in the second Landau level due to a strong coupling of the orbital motion.

Indeed, experimental attempts [75,76,47,18,56,54] under this approach have shown surprisingly complex behaviors. First, it was observed [75,76] that the in-plane magnetic field from tilting can induce a phase transition from the quantum Hall effect phase to an anisotropic phase in the second Landau level. Then, the mixing of different electric subbands under tilt can give rise to totally different tilt magnetic field dependence of the 7/3 and 8/3 energy gaps in samples of different well width [54], thus making asserting their spin polarization almost impossible.

In this section, we use a different approach and study the spin polarization of the 7/3 and 8/3 states as a function of electron density (n). Under this approach, the B-field is always perpendicular to the two-dimensional electron system (2DES). By changing the 2DES density, the ratio of Coulomb energy E_c to the Zeeman energy E_z also changes, since $E_c \sim n^{1/2}$ and $E_z \sim n$. In this regard, the density dependence approach is equivalent to tilting magnetic field but it cannot cause a tilt-field induced phase transition. It is observed that in the density range between 0.5×10^{11} and 3×10^{11} cm^{-2}, the energy gap of the 8/3 state ($\Delta_{8/3}$) first decreases with increasing density, nearly disappears at $n \sim 0.8\times10^{11}$ cm^{-2}. Beyond this density, $\Delta_{8/3}$ increases with increasing density. This density dependence of $\Delta_{8/3}$ clearly signals a spin transition at this filling factor. For comparison, the energy gap of the 7/3 state ($\Delta_{7/3}$) shows a monotonic density dependence, supporting a spin polarized state down to 0.5×10^{11} cm^{-2}.

Table I. The quantum well width (W), 2DES density and mobility, as well as the magnetic length (l_B) at ν=8/3 and the ratio of W/l_B for the samples studied in this work.

samples	well width (nm)	density (10^{11} cm^{-2})	mobility (10^6/V s)	l_B at ν=8/3 (nm)	W/l_B
A	60	0.5	10	29.2	2.1
B	60	0.6	9.1	26.7	2.2
C	56	0.77	13	23.6	2.4
D	45	1.15	13.8	19.3	2.3
E	33	2.1	23	14.3	2.3
F	30	2.6	24	12.9	2.3
G	30	3.1	31	11.8	2.5

The specimens we used in this study are a series of high quality symmetrically doped GaAs quantum wells. Table I lists the sample parameters, including the 2DES density, mobility, and quantum well width (W), and the ratio of W/l_B at the Landau level filling ν=8/3. The low-temperature electron density and mobility were established by a brief red light-emitting diode illumination at 4.2K. Standard low-frequency lock-in technique (~ 11Hz) was utilized to measure the magnetoresistance R_{xx} and Hall resistance R_{xy}.

In Figure 8a, we show the R_{xx} trace for sample C. A fully developed 5/2 state is clearly seen at B ~ 1.3T, i.e., vanishingly small R_{xx} and a quantized R_{xy} (not shown). This is so far the lowest B field that a fully developed 5/2 FQHE state has been reported. R_{xx} minimum is also observed at other filling factors ν=7/3, 8/3, 11/5, and 14/5. In Fig.8b, a

semi-log plot of R_{xx} versus 1/T is shown for ν=8/3 and 7/3. From fitting, the energy gaps at these two fillings are obtained: $\Delta_{7/3}$ ~ 35 mK and $\Delta_{8/3}$ ~ 10 mK.

In Fig. 8c, we show the R_{xx} trace at a lower electron density of $n=0.5\times10^{11}$ cm^{-2}. In this lower density sample, only the strongest FQHE states at ν=8/3, 5/2, and 7/3 are seen. What is really surprising is that the 8/3 state is the strongest among the three FQHE states. This is also corroborated when examining their activation energy gaps (shown in Fig.8d): $\Delta_{7/3}$ ~ 5 mK and $\Delta_{8/3}$ ~ 45 mK.

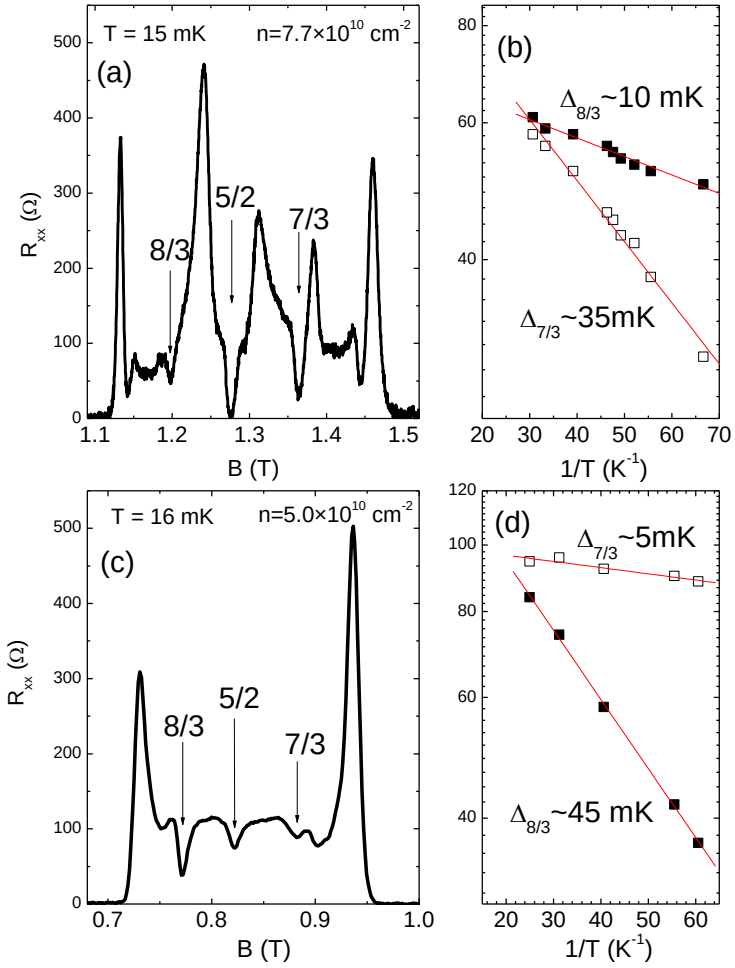

Figure 8: Magneto-resistance R_{xx} for sample C (Fig. 8a) and A (Fig. 8c). Arrows mark the positions of the FQHE states at ν=8/3, 5/2, and 7/3. Fig. 8b and Fig. 8d show the temperature dependence of R_{xx} at ν=8/3 (filled squares) and 7/3 (open squares) in these two samples, respectively. The lines are linear fit.

In Figure 9a and 9b, we plot the energy gaps at ν=8/3 and 7/3 as a function of electron density. It is clear that the energy gap of the 8/3 state first decreases with increasing density, nearly disappears at $n \sim 0.8\times10^{11}$ cm^{-2}. Beyond this density, $\Delta_{8/3}$ increases with

increasing density. This change observed in the 8/3 energy gap is very similar to what was observed in the ν=2/3 FQHE in the lowest Landau level [77,78] and demonstrates a spin transition [77-85] from a spin unpolarized ground state at low densities to a spin polarized one at higher densities. For comparison, $\Delta_{7/3}$ shows a monotonic density dependence, supporting that the 7/3 state is spin-polarized down to 0.5×10^{11} cm^{-2}.

Before we discuss the implications of the above observation, we want to point out that the observed spin transition is intrinsic and cannot be induced by extrinsic means, such as finite thickness [86] or Landau level mixing [87]. First, it has been shown that the spin polarization of a FQHE state is insensitive to the finite-thickness correction [71]. Second, in this experiment, the quantum well width is varied in accordance with the electron density so that the parameter, W/l_B, a measure of effective thickness of 2DES, remains more or less the same in all samples, as shown in Table I. Consequently, the percentage of the reduction to the energy gap calculated for an ideal 2DEG is roughly the same for all the samples. The Landau level mixing (LLM) effect cannot cause the above spin transition, either. It is known that LLM is strong at low electron densities [87]. As a result, the reduction of energy gap due to LLM should be larger at low densities, actually smearing the sharpness of transition if the intrinsic gap were plotted.

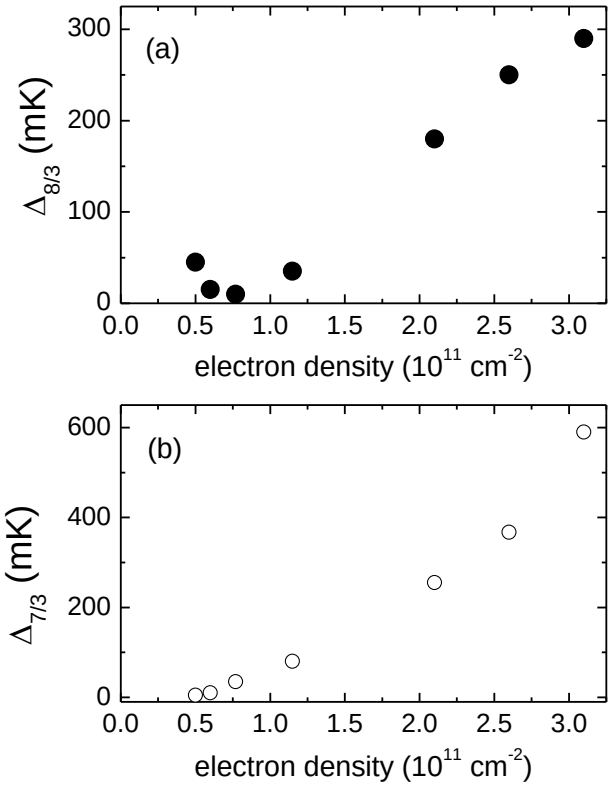

Figure 9: Activation energy gap at ν=8/3 (a) and 7/3 (b) as a function of density.

In a recent publication, Liu et al showed there exists a giant enhancement in the 5/2 energy gap in the vicinity of the crossing between Landau levels belonging to the different (symmetric and antisymmetric) electric subbands [55]. A self consistent calculation for our samples has ruled out this possibility for a large ν=8/3 energy gap in the low density regime.

The observation of a spin transition at 8/3 is contradictory to the conclusion reached in Ref. [71], where the authors found from their numerical calculation that the 8/3 state was different from the 2/3 state and remained spin polarized even at vanishingly small Zeeman energy. This is, as they argued, because the more repulsive effective interactions in the second Landau level force electrons to occupy the maximum spin state. Our experimental results, however, show that the 8/3 state behaves very much like the 2/3 state and display a spin transition as a function of density. One may argue that the theoretical calculation was carried out at a 2DES density of ~ 2.8×10^{11} cm^{-2}, which is much larger than the transition density of 0.8×10^{11} cm^{-2}. On the other hand, the relevant parameter in determining the spin polarization of a FQHE state is the ratio of the Zeeman energy E_z to Coulomb energy E_c [88]. At $n=0.5\times10^{11}$ cm^{-2}, E_z/E_c ~ 0.005. Using the parameters quoted in Ref. [71], $n=2.8\times10^{11}$ cm^{-2} and g*=0.05, E_z/E_c is much smaller, ~ 0.0015. Thus, the 8/3 state considered in Ref. [71] should be deeper in the unpolarized regime, instead of being fully polarized predicted by the theoretical calculations.

A spin unpolarized ground state at ν=8/3 is also inconsistent with the models of a spin-polarized non-Abelian state for the 3rd FQHE states in the second Landau level. On the other hand, it remains unclear whether it can be a two-component non-Abelian state [70], or a paired spin-singlet quantum Hall state [67], or a boundary state between the Abelian and non-Abelain states [69]. Our current data are not able to address this question.

The observation of a spin transition at 8/3 and a spin polarized 7/3 state, on the other hand, is mostly consistent with the composite fermion model with a spin [49]. This can be derived from a simple analogy of their counterparts in the first Landau level. Under the CF model, the 7/3 state is mapped onto the ν^*=1 interger quantum Hall effect (IQHE) state of the CFs emanating from the 1/2 state in the second Landau level and, thus, is spin polarized. The 8/3 state is the ν^*=2 IQHE sate of the CFs and is spin unpolarized at small effective magnetic fields, or low electron densities. With increasing density, CF Landau level crossing can occur [49] and the 8/3 state becomes spin-polarized beyond the critical density.

One remark is in order before we conclude this paper. Unlike in the high density regime where $\Delta_{7/3}$ is roughly twice of $\Delta_{8/3}$, at $n=0.5\times10^{11}$ cm^{-2} $\Delta_{7/3}$ is much smaller than $\Delta_{8/3}$. In fact, $\Delta_{8/3} \sim 10 \times \Delta_{7/3}$. This big difference probably can be explained under the CF model with a spin, where the energy gap at ν^*=1 or ν=7/3 is due to Zeeman splitting of CFs and the energy gap at ν^*=2 or ν=8/3 is due to cyclotron gap. Alternatively, it is possible that the 7/3 state may also be spin unpolarized at even lower electron densities than studied in this experiment, and the spin transition occurs very close to 0.5×10^{11} cm^{-2}, where a tiny 7/3 gap was observed. On the other hand, a spin-unpolarized 7/3 state is not expected under the CF picture.

In summary, we have carried out density dependence of the energy gaps at ν=8/3 and 7/3 in a series of high quality quantum wells. A spin transition is observed in the 8/3 FQHE. The 7/3 state appears to be spin polarized down to 0.5×10^{11} cm^{-2}.

5. EDGE CHANNEL TUNNELING SPECTROSCOPY OF 5/2 FRACTIONAL QUANTUM HALL EXCITATIONS IN ETCH DEFINED QUANTUM POINT CONTACTS

Ever since its discovery the fractional quantum Hall (FQH) state at the even denominator filling-fraction 5/2 has triggered a number of theoretical and experimental studies [3,4]. There is also a renewed interest in the study of 5/2 state due to the proposed fault-tolerant topological quantum computation, which is based on a system obeying non-Abelian statistics [7,89-91]. The prevailing understanding is that the 5/2 state consists of composite-Fermion pairs condensed into a BCS like ground state. Within this interpretation the ground state excitations or the quasiparticles of 5/2 state posses' non-Abelian statistics and associated topological properties. More over quasiparticles of 5/2 states are energetically separated from the excited states. Based on this energy separation theory predicts an error rate of $< 10^{-30}$ for the 5/2 state based topological qubits, far superior to other candidates for qubits in terms of error-free computation [7]. If proved non-Abelian, quasiparticles of 5/2 state will provide a clean and simple system for the realization of topological qubits.

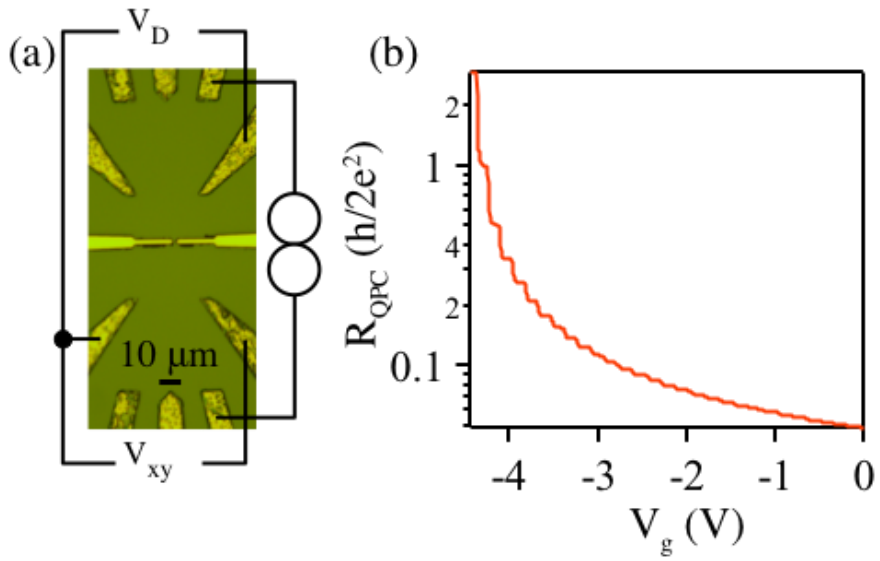

Fig. 10: (a) Optical micrograph of a representative QPC device with a schematic diagram of the measurement setup superposed. (b) R_{QPC} as a function of gate voltage V_g showing well defined quantized conductance plateaus.

The excitations of a quantum Hall state are chiral Luttinger liquid propagating along the edges of the sample whose direction of propagation is defined by the Lorentz-force direction. Physics of these edge channels can be probed by allowing the edge states to interact with each other. These interactions are nonexistent in bulk samples due to the large separation between the edges. In samples with confined geometries such as quantum point contacts (QPC) these edge-states can be brought together facilitating inter-edge interactions. Theoretically proposed studies utilize inter-edge tunneling of quasiparticles as tool to study their properties [92] . There have been a few experimental efforts to study the quasiparticles of 1/3 filling-fraction [93-94], not much

attempts to study 5/2 state in confined geometries[16,95]. This is partially due to the fact that unlike other states 5/2 state is very fragile and can be observed only in samples with highest quality. In this work we report formation of 5/2 FQH state in a QPC defined on a high mobility GaAs/AlGaAs two dimensional electron gas. We conduct tunneling experiments of quasiparticles in this QPC and, from the temperature and the bias dependence of tunneling conductance, we obtain the effective charge and Coulomb interaction parameters.

Our device consist of a QPC formed on a GaAs/AlGaAs heterostructure with a surface carrier concentration $n_s \sim 1.6 \times 10^{11}/cm^2$ and a mobility $\mu \sim 15 \times 10^6$ cm^2/Vs. Fig. 10 (a) shows an optical micrograph of a representative device. There are five ohmic contacts on either side of the QPC defined by optical lithography followed by Ni/Au/Ge/Ni/Au deposition and high temperature annealing. QPCs are generally fabricated by electron-beam lithography. Even though finer control of the geometrical size of the devices can be achieved, during electron-beam lithography the material properties tend to degrade. Formation of 5/2 FQH state is very sensitive to the quality of the material and here we utilize an all-optical lithography process to fabricate our device to preserve the heterostructure quality. The QPC gates are defined by optical lithography followed by dry etching and deposition of Cr/Au Schottky gates. The etch defines the constriction without applying any gate voltage and helps to maintain a uniform electron density and filling-fraction around the constriction. In the absence of the etch one will have to apply a very low gate-voltage to create the constriction causing a non-uniform electron density profile in the vicinity.

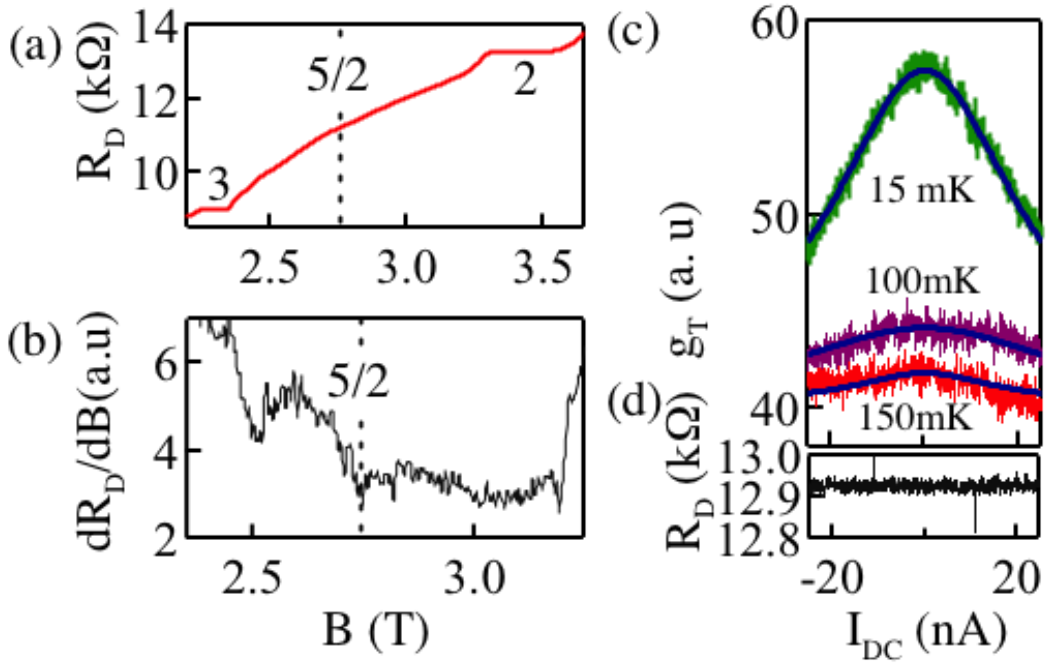

Fig. 11: ν =5/2 FQH state in QPC: (a) R_D vs B field showing the ν =3, 5/2 and 2 plateaus. (b) Numerical derivative of the data shown in (a) vs B field. The dip at B = 2.73 T correspond to 5/2 FQH state. (c) g_T vs DC source drain bias current I_{DC} for 15 mK (green), 100 mK (magenta) and 150 mK (red) sample temperatures. Blue curves represent the global fit to the data using the weak-tunneling formula. (d) R_D vs I_{DC} for B = 3.25T corresponding to the 2nd Landau level.

All the measurements were carried out in the milli-Kelvin temperature range in a dilution refrigerator. Standard four-probe lock-in technique in the AC or AC+DC mode is used for all the measurements. A schematic diagram of the measurement setup is given in Fig. 10 (a). The Hall voltage V_{xy} and the diagonal voltage V_D are measured simultaneously. Fig 10 (b) is a plot of the QPC resistance as function of gate voltage V_g. Well formed steps in units of resistance quantum starting from zero gate voltage down to the complete pinch-off of the channel is a signature of a well-defined QPC.

Fig. 11 (a) shows a plot of $R_{D,}$ the diagonal differential resistance across the QPC as a function of magnetic field B normal to the sample showing integer quantum Hall plateaus corresponding to the filling-fractions $\nu = 2$ and $\nu = 3$. The plateau around B = 2.73 T correspond to $\nu = 5/2$ filling-fraction. For a better visibility we take numerical derivative of the data in Fig. 11 (a) and is given in Fig. 11 (b). A well-defined dip at B = 2.73 T corresponds to the formation of 5/2 state.

Next, we discuss tunneling experiments in the QPC at $\nu = 5/2$ filling-fraction [Fig. 11 (c)]. In these experiments both the Hall resistance R_{xy} and the diagonal resistance R_D across the QPC are measured simultaneously as shown in Fig. 10 (a). The tunnel conductance $g_T = R_D - R_{xy}/R_{xy}^2$ reflects the contribution to the total conductance due to the quasiparticles tunneling between the edge channels at the constriction. The green curve in Fig 11. (c) represents g_T as a function of DC source-drain bias current at B = 2.73 T, corresponding to the $\nu = 5/2$ FQH state, at 15mK. The peak centered at zero bias is a signature of quasiparticle tunneling. Fig 11. (d) represents a similar measurement of R_D at B = 3.25 T, on the $\nu = 2$ integer quantum Hall plateau. The ground state at $\nu = 5/2$ consists of quasiparticles whereas the ground state at $\nu = 2$ consists of electrons. The absence of any peak for $\nu = 2$ and the presence of a zero bias peak at $\nu = 5/2$ implies that the tunneling is due to the quasiparticles [93]. This also confirms that tunneling happens only between the top-most counter-propagating edge-states and, our device is in the weak-tunneling regime.

Weak tunneling between counter-propagating edge-channels in constrictions has been proposed as a tool to study quasiparticles properties long back [92,96] and, has been experimentally studied in the recent past [93,95]. According to the theory, the tunneling conductance g_T is a strong function of the potential difference between the counter propagating edges and also of the temperature and is given by the formula

$$g_T = g_T^0 + AT^{(2g-2)}F\left(\frac{e^* V_D}{k_B T}, g\right) \quad \text{where,}$$

$$F(x,g) = B\left(g + i\frac{x}{2\pi}, g - i\frac{x}{2\pi}\right)\left\{\left\{\pi\cosh\left(\frac{x}{2}\right) - 2\sinh\left(\frac{x}{2}\right)\mathrm{Im}\left[\Psi\left(g + i\frac{x}{2\pi}\right)\right]\right\}\right\}.$$

Where, A is the amplitude, V_D is the potential difference between the counter propagating edge states, T is the temperature, Ψ is the digamma function and B is the beta function. In the quantum Hall regime $V_D = R_H I_{DC}$.

Fig. 11 (c) shows quasiparticles tunneling conductance for $\nu = 5/2$ filling-fraction as a function of DC source-drain bias current I_{DC} for three sample temperatures, 15 mK, 100 mK and, 150 mK. The tunneling I-g_T curves are consistent with the expression for weak tunneling of quasiparticles.

A global fit to the data using the expression is also given in Fig. 11 (c) [blue curves]. For the fits A, g and g_T^0 are kept as free parameters. e* is kept ¼. From the fits we obtain Coulomb interaction parameter g = 0.7.

In conclusion we have fabricated QPC devices on a high mobility GaAs/AlGaAs heterostructure. We observe well-defined quantized plateaus in the QPC conductance. We have observed FQH plateau corresponding to the $\nu = 5/2$ filling-fraction. We have conducted tunneling experiments enabling us to characterize the quasiparticles properties.

6. SUMMARY AND OUTLOOK

This LDRD was successful in studying the physics of the 5/2 fractional quantum Hall effect state, a leading contender for realizing topological quantum computation. First, we have examined the impact of different kind of disorders on the experimental 5/2 energy gap. We observe that in modulation doped quantum well samples where disorder is dominated by the long-range Coulombic fluctuations the 5/2 energy gap decreases quickly with increasing $1/\mu$ or disorder. On the other hand, in HIGFETs, where the disorder is dominantly due to short-range surface roughness fluctuations, the 5/2 energy gap shows a weak mobility dependence. Moreover, our density dependent result of the 5/2 energy gap is consistent with a spin polarized 5/2 state and deviate considerable from a description in terms of a spin-unpolarized state.

Second, we have carried out tilt magnetic field dependent studies of the 12/5 fractional quantum Hall effect state. Its diagonal magneto-resistance R_{xx} shows a non- monotonic dependence on tilt angle, and displays a maximum at $\theta \sim 14°$. We show that this tilt dependence can be understood within the model of CFs with a spin, with appropriate m* and g* values assumed. Furthermore, correlated with the tilt dependence of R_{xx} and R_{yy}, the 12/5 activation energy $\Delta_{12/5}$ also shows a non-monotonic B dependence. This tilt B dependence of R_{xx} and $\Delta_{12/5}$ is in striking difference from that of the well-documented 5/2 state and, thus, calls for more investigations of the nature of the 12/5 FQHE.

Third, we have carried out density dependence of the energy gaps at ν=8/3 and 7/3 in a series of high quality quantum wells. A spin transition is observed in the 8/3 FQHE. The 7/3 state appears to be spin polarized down to 0.5×10^{11} cm^{-2}.

Finally, we have fabricated QPC devices on a high mobility GaAs/AlGaAs heterostructure. We observe well-defined quantized plateaus in the QPC conductance. We have observed FQH plateau corresponding to the ν = 5/2 filling-fraction. We have conducted tunneling experiments enabling us to characterize the quasiparticles properties.

In terms of outlook, what was written in an internal report prepared several years ago is still relevant. There are several proposed ways in which a topological quantum computer could operate using the 5/2 state. Each measures the state of qubits by measuring the interference around a loop, or cell, which encloses the anyons to be measured. Techniques for performing qubit gates include an edge-state approach, which uses single particles on the edge of the FQHE state to braid with localized anyons contained in cells, and a measurement-only approach, which uses a series of measurements on localized anyons to braid the anyons. The edge-state approach requires precise timing of control electronics, but can be implemented using a standard quantum hall device structure. The measurement-only approach requires a more complex device structure, but has the advantage that all braids can be performed and less precision is needed in the controlling electronics. In either case, braiding alone cannot implement all the qubit gates necessary for universal quantum computation, and additional non-topologically-protected gates must be used. Fortunately, these non-protected gates can be quite noisy as long as a large number of qubits can be implemented. More specifically, there is a tradeoff between the number of "overhead" qubits (in addition to the number of logical qubits required for a computation) that are required and the intrinsic error of the non-protected gates.

In order to implement the proposed experiments to measure quasiparticle properties and later encode qubits, real devices will need to be fabricated on high mobility GaAs heterostructures that are consistent with preserving the quality of the 2D electron system and the high energy gap of the $\nu=5/2$ quantum Hall state. Existing processing techniques are reviewed, and fabrication requirements to create complicated topological quantum computing cells are discussed. For single cells, more complicated gate patterns using strips, anti-dots in the cell and tunnel barrier and grids of gates, called pixel gates, allows enough flexibility to implement many of the intermediate experiments and both the edge-state and measurement-only approaches to TQC. Even a single qubit, however, will require more than one cell. A linear chain of cells with the appropriate gates and ohmic contacts is considered that is consistent with internal anti-dots and the more complicated gate patterns for the single cells. As multiple cells in this linear chain are operated, access to ohmic contacts will require some gates to cycle local densities from the "bulk" density at 5/2 to complete depletion.

7. REFERENCES

[1] D.C. Tsui, H.L. Stormer, A.C. Gossard, Phys. Rev. Lett. **48**, 1559 (1982).
[2] R.B. Laughlin, Phys. Rev. Lett. **50**, 1395 (1983).
[3]. R.L. Willett, J.P. Eisenstein, H.L. Stormer, D.C. Tsui, A.C. Gossard, and J.H. English, Phys. Rev. Lett. **59**, 1779 (1987).
[4] W. Pan, J.-S. Xia, V. Shvarts, E.D. Adams, H.L. Stormer, D.C. Tsui, L.N. Pfeiffer, K.W. Baldwin, and K.W. West, Phys. Rev. Lett. **83**, 3530 (1999).
[5] G. Moore and N. Read, Nucl. Phys. B **360**, 362 (1991).
[6] M. Greiter, X.G. Wen, and F. Wilczek, Phys. Rev. Lett. **66**, 3205 (1991).
[7] C. Nayak, S.H. Simon, A. Stern, M. Freedman, and S. Das Sarma, Rev. Mod. Phys. **80**, 1083 (2008).
[8] G.S.Boebinger, H.L. Stormer, D.C. Tsui, A.M. Chang, J.C.M. Hwang, A.Y. Cho, C.W. Tu, and G. Weiman, Phys. Rev. B **36**, 7919(1987).
[9] X. Wan, D.N. Sheng, E.H. Rezayi, K. Yang, R.N. Bhatt, and F.D.M. Haldane, Phys. Rev. B **72**, 075325 (2005).
[10] Wanli Li, et al, Phys. Rev. Lett. **94**, 206807 (2005); Phys. Rev. Lett. **102**, 216801 (2008); Phys. Rev. B **81**, 033305 (2010).
[11] B.E. Kane, L.N. Pfeiffer, K.W. West, and C.K. Harnett, Appl. Phys. Lett. **63**, 2132 (1993).
[12] F. Stern and W.E. Howard, Phys. Rev. **163**, 816 (1967).
[13] W. Pan, H.L. Stormer, D.C. Tsui, L.N. Pfeiffer, K.W. Baldwin, and K.W. West, solid State Communications **119**, 641 (2001).
[14] W. Pan, J. S. Xia, H. L. Stormer, D. C. Tsui, C. Vicente, E. D. Adams, N. S. Sullivan, L. N. Pfeiffer, K. W. Baldwin, and K. W. West, Phys. Rev. B **77**, 075307 (2008).
[15] J.P. Eisenstein, K.B. Cooper, L.N. Pfeiffer, and K.W. West, Phys. Rev. Lett. **88**, 076801 (2002).
[16] J. B. Miller, I. P. Radu, D. M. Zumbuhl, E. M. Levenson-Falk, M. A. Kastner, C.M. Marcus, L. N. Pfeiffer, and K.W. West, Nature Phys. **3**, 561 (2007).
[17] H.C. Choi, W. Kang, S. Das Sarma, L.N. Pfeiffer, K.W. West, Phys. Rev. B, **77**, 081301 (2008).
[18] C. R. Dean, B. A. Piot, P. Hayden, S. Das Sarma, G. Gervais, L. N. Pfeiffer, and K. W. West, Phys. Rev. Lett. **100**, 146803 (2008).
[19] J. Nübler, V. Umansky, R. Morf, M. Heiblum, K. von Klitzing, and J. Smet, Phys. Rev. B **81**, 035316 (2010).
[20] A. Kumar, M.J. Manfra, G.A. Csáthy, L.N. Pfeiffer, and K.W. West, Phys. Rev. Lett. **105**, 246808 (2010).
[21] Z. Papić, N. Regnault, and S. Das Sarma, Phys. Rev. B **80**, 201303 (2009).
[22] J.K. Jain, Phys. Rev. Lett. **63**, 199 (1989).
[23] B.I. Halperin, P.A. Lee, and N. Read, Phys. Rev. B **47**, 7312 (1993).
[24] S.V. Syzranov, I.L. Aleiner, B.L. Altshuler, and K.B. Efetoc, Phys. Rev. Lett. **105**, 1370001 (2010)
[25] V. Umansky, M. Heiblum, Y. Levinson, J. Smet, J. Nübler, M. Dolev, J. Cryst. Growth **311**, 1658 (2009).
[26] G. Gamez and K. Muraki, preprint, arXiv:1101.5856v1 (2011).
[27] D. Yoshioka, Surface Science **170**, 125 (1980).
[28] S.M. Girvin, A.H. MacDonald, and P.M. Platzman, Phys. Rev. Lett. **54**, 581 (1985).

[29] K. Park and J.K. Jain, Solid State Communication **115**, 353 (2000).
[30] M.R. Peterson, Th. Jolicoeur, and S. Das Sarma, Phys. Rev. Lett. **101**, 016807 (2008).
[31] W. Bishara and C. Nayak, Phys. Rev. B **80**, 121302 (2009).
[32] A. Wójs, C. Tőke, and J.K. Jain, Phys. Rev. Lett. **105**, 096802 (2010).
[33] N. Read and E. Rezayi, Phys. Rev. B **59**, 8084 (1999).
[34] E. Ardonne and K. Schoutens, Phys. Rev. Lett. **82**, 5096 (1999).
[35] S.H. Simon *et al.*, Phys. Rev. B **75**, 075317 (2007).
[36] W. Bishara, G.A. Fiete, and C. Nayak, Phys. Rev. B **77**, 241306 (2008).
[37] P. Bonderson and J.K. Slingerland, Phys. Rev. B **78**, 125323 (2008).
[38] B.A. Bernevig and F.D.M. Haldane, Phys. Rev. Lett. **101**, 246806 (2008).
[39] E.H. Rezayi and N. Read, Phys. Rev. B **79**, 075306 (2009).
[40] M. Levin and B.I. Halperin, Phys. Rev. B **79**, 205301 (2009).
[41] M.V. Milovanović, Th. Jolicoeur, and I. Vidanović, Phys. Rev. B **80**, 155324 (2009).
[42] M. Barkeshli and X.G. Wen, Phys. Rev. B **84**, 115121 (2011).
[43] G.J. Sreejith *et al.*, Phys. Rev. Lett. **107**, 086806 (2011).
[44] M. Freedman, M. Larsen, and Z. Wang, Comm. Math. Phys. **227**, 105 (2002).
[45] L. Hormozi, N.E. Bonesteel, and S.H. Simon, Phys. Rev. Lett. **103**, 160501 (2009).
[46] J.S. Xia *et al.*, Phys. Rev. Lett. **93**, 176809 (2004).
[47] G.A. Csáthy *et al.*, Phys. Rev. Lett. **94**, 146801 (2005).
[48] S.Y. Lee, V.W. Scarola, and J.K. Jain, Phys. Rev. B **66**, 085336 (2002).
[49] R. R. Du, A. S. Yeh, H. L. Stormer, D. C. Tsui, L. N. Pfeiffer, and K. W. West, Phys. Rev. Lett. **75**, 3926 (1995).
[50] J.P. Eisenstein *et al.*, Phys. Rev. Lett. **62**, 1540 (1989).
[51] W. Kang *et al.*, Phys. Rev. **56**, 12776 (1997).
[52] W. Pan *et al.*, Phys. Rev. B **61**, 5101 (2000).
[53] A.S. Yeh *et al.*, Phys. Rev. Lett. **82**, 592 (1999).
[54] J. Xia *et al.*, Nature Physics **7**, 845 (2011).
[55] Y. Liu *et al.*, Phys. Rev. Lett. **107**, 176805 (2011).
[56] C. Zhang *et al.*, Phys. Rev. Lett. **104**, 166801 (2010).
[57] J.K. Jain, Phys. Rev. Lett. **63**, 199 (1989).
[58] A. Lopez and E. Fradkin, Phys. Rev. B **44**, 5246 (1991).
[59] B.I. Halperin, P.A. Lee, and N.Read, Phys. Rev. B **47**, 7312 (1993).
[60] L. Tiemann, G. Gamez, N. Kumada, and K. Muraki, Science **335**, 828 (2012).
[61] M. Stern, B.A. Piot, Y. Vardi, V. Umansky, P. Plochocka, D.K. Maude, and I. Bar-Joseph, Phys. Rev. Lett. **108**, 066810 (2012).
[62] F.D.M. Haldane, Phys. Rev. Lett. **51**, 605 (1983).
[63] B.I. Halperin, Phys. Rev. Lett. **52**, 1583 (1984).
[64] J.K. Jain, Physics **3**, 71 (2010).
[65] A.H. MacDonald and S.M. Girvin, Phys. Rev. B **33**, 4009 (1986).
[66] N. d'Ambrumenil and A.M. Reynolds, J. Phys. C **21**, 119(1988).
[67] E. Ardonne, F. J. M. van Lankvelt, A. W. W. Ludwig, and K. Schoutens, Phys. Rev. B **65**, 041305 (2004).
[68] N. Regnault, M.O. Goerbig, and Th. Jolicoeur, Phys. Rev. Lett. **101**, 066803 (2008).
[69] A. Wojs, Phys. Rev. B **80**, 041104 (2009).
[70] M. Barkeshli and X.G. Wen, Phys. Rev. B **82**, 233301 (2010).
[71] T. Chakraborty and P. Pietilainen, Phys. Rev. Lett. **83**, 5559 (1999).

[72] R.G. Clark, S.R. Haynes, A.M. Suckling, J.R. Mallett, P.A. Wright, J.J. Harris, and C.T. Foxon, phys. Rev. Lett. **62**, 1536 (1989).
[73] J.P. Eisenstein, H.L. Stormer, L.N. Pfeiffer, and K.W. West, Phys. Rev. Lett. **62**, 1540 (1989).
[74] A.G. Davies, R. Newbury, M. Pepper, J.E.F. Frost, D.A. Ritchie, and G.A.C. Jones, Phys. Rev. B **44**, 13128 (1991).
[75] W. Pan, R.R. Du, H.L. Stormer, D.C. Tsui, L.N. Pfeiffer, K.W. Baldwin, and K.W. West, Phys. Rev. Lett. **83**, 820 (1999).
[76] M.P. Lilly, K.B. Cooper, J.P. Eisenstein, L.N. Pfeiffer, and K.W. West, Phys. Rev. Lett. **83**, 824 (1999).
[77] J.P. Eisenstein, H.L. Stormer, L.N. Pfeiffer, and K.W. West, Phys. Rev. B **41**, 7910 (1990).
[78] L.W. Engel, S.W. Hwang, T. Sajoto, D.C. Tsui, and M. Shayegan, Phys. Rev. B **45**, 3418 (1992).
[79] J.H. Smet, R.A. Deutschmann, W. Wegscheider, G. Abstreiter, and K. von Klitzing, Phys. Rev. Lett. **86**, 2412 (2001).
[80] N. Freytag, Y. Tokunaga, M. Horvatic, C. Berthier, M. Shayegan, and L.P. Levy, Phys. Rev. Lett. **87**, 136801 (2001).
[81] K. Hashimoto, K. Muraki, T. Saku, and Y. Hirayama, Phys. Rev. Lett. **88**, 176601 (2002).
[82] R. Chughtai, V. Zhitomirsky, R.J. Nicholas, and M. Henini, Phys. Rev. B **65**, 161305 (2002).
[83] F. Schulze-Wischeler, E. Mariani, F. Hohls, and R.J. Haug, Phys. Rev. Lett. **92**, 156401 (2004).
[84] V.S. Khrapai, A.A. Shashkin, M.G. Trokina, V.T. Dolgopolov, V. Pellegrini, F. Beltram, G. Biasiol, and L. Sorba, Phys. Rev. Lett. **99**, 086802 (2007).
[85] B. Verdene, J. Martin, G. Gamez, J. Smet, K. von Klitzing, D. Mahalu, D. Schuh, G. Abstreiter, and A. Yacoby, Nature Phys. **3**, 392 (2007).
[86] M. Peterson, Th. Jolicoeur, and S. Das Sarma, Phys. Rev. B **78**, 155308 (2008).
[87] A. Wojs and J.J. Quinn, Phys. Rev. B **74**, 235319 (2006).
[88] N. Shibata and K. Nomura, J. Phys. Soc. Japn. **76**, 103711 (2007).
[89] G. P. Collins, Scientific American **294**, 56-63 (2006).
[90] S. Das Sarma, M. Freedman, and C. Nayak, Phys. Rev. Lett. **94**, 166802 (2005).
[91] A. Yu. Kitaev, Annals of Physics **303**, 2-30 (2003).
[92] X.-G. Wen, Phys. Rev. B **44**, 5708-5719 (1991).
[93] S. Roddaro, V. Pellegrini, F. Beltram, G. Biasiol, L. Sorba, R. Raimondi, and G. Vignale, Phys. Rev. Lett. **90**, 046805 (2003).
[94] S. Roddaro, V. Pellegrini, F. Beltram, L. N. Pfeiffer, and K. W. West, Phys. Rev. Lett. **95**, 156804 (2005).
[95] I. P. Radu, J. B. Miller, C. M. Marcus, M. A. Kastner, L. N. Pfeiffer, and K. W. West, Science **320**, 899 -902 (2008).
[96] C. L. Kane and M. P. A. Fisher, in *Perspectives in Quantum Hall Effects: Novel Quantum Liquids in Low-Dimensional Semiconductor Structures* (John Wiley & Sons, Inc, 1997), pp. 109-159.

[Blank page following section.]

DISTRIBUTION

1	MS0359	D. Chavez, LDRD Office	1911
1	MS0899	Technical Library	9536 (electronic copy)
1	MS1086	Jeff Cederberg	1126
1	MS1086	Matthew Crawford	1733
1	MS1086	Wei Pan	1121
1	MS1415	Erik Nielsen	1121
1	MS1415	Xiaoyan Shi	1121
1	MS1421	Daniel Barton	1121
1	MS1421	Jerry Simmons	7000


Sandia National Laboratories